International Journal of Multidisciplinary Research and Development
www.allsubjectjournal.com
Online ISSN: 2349-4182, Print ISSN: 2349-5979
Received: 05-11-2021, Accepted: 21-11-2021, Published: 06-12-2021
Volume 8, Issue 12, 2021, Page No. 23-32

Modification of chitosan/carboxymethyl cellulose composite with glutaraldehyde and ethylene diamine for the removal of Cr (VI) from aqueous solutions

Rafia Sharif[1], Essa Esmail Mohammad Ahmed[2], Mohammed Al-Bushra Hassan[3], Late Muhammed Ali Hussain[4]
Department of Chemistry, International University of Africa, Khartoum, Sudan
Department of Chemistry, Sudan University, Khartoum, Sudan

Abstract

In this work the chitosan/carboxymethyl cellulose (CMC) composite was modified by reacting chitosan/CMC composite with glutaraldehyde (GA) and ethylene diamine (EA) as a cross linker. The different amounts of chitosan/CMC composite as well as different volumes of distilled water were used to prepare the modified composite samples. The resultant composites were used to remove Cr (VI) from standard aqueous solution. The modified composite was characterized by the FT-IR, SEM and TGA. The optimum conditions for adsorption of Cr (VI) on modified composite were found at pH range of 2.0-4.0 and stirring time of 7 minutes. Kinetic study results showed that the adsorption process follows pseudo-second order model, while the Langmuir adsorption isotherm provide the best fit with a maximum adsorption capacity from 33.77 to 89.24 mg/g at $25^{o}C$, indicating that the rate limiting step in the absorption of Cr (VI) involves the best physical interaction physisorption. Thermodynamic parameters in TGA analysis indicated an endothermic process and spontaneous adsorption of Cr (VI) on the polymers. Results from this work demonstrated that the prepared composite possess great potential for removing Cr (VI) from contaminated or waste water.

Keywords: bio-composites, physisorption, glutaraldehyde and ethylene diamine cross-linker, Pseudo-second order Kinetic, Langmuir adsorption isotherm

Introduction

Chitosan is a modified natural cationic polymer composed of β-(1→4)-linked D-glucosamine residues, obtained by partial N-deacetylation of chitin. This polyaminosaccharide polymer has polycationic characteristics, due to the presence of numerous amino groups, [1] that's why in recent days, the chitosan is in greatest used. Chitosan is biodegradable, economic and environmental friendly adsorbent with its promising properties for the adsorption of heavy metals from an aqueous media make it more useful to build the multilayer structure for the adsorption purpose [2, 3]**.** The modification of Chitosan/CMC Composite from different methods (physical and chemical) considered as the most favorable composite for the adsorption of heavy metal from the aqueous media [4]. Heavy metals, such as Cd (II) and Cr (VI), cause water pollution and serious impact on the human health. The chromium present as CrO^{4-}chromate and $Cr_2O_7^{2-}$ dichromate anions and because of great solubility of Chromium in water, the chromium Cr (VI) is very toxic to organisms, and even carcinogenic [5]. Bio composites of natural polymer like Chitosan and CMC can be modified chemically by introducing cross-linker like glutraldehyde, ethylene diammine, glyoxal, formaldehyde, and epichlorohydrin. The chemical groups of these cross-linkers could be capable of interacting with the pollutant [6]. According to few research papers the adsorption properties of chitosan is due to the presence of different functional groups a position in its chemical structure. The modification of chitosan, either with the grafting or cross-linking reactions, the resultant chitosan derivatives enhance the adsorption capacity. In the case of grafting reactions, the addition of extra functional groups onto chitosan increases the number of adsorption sites and also the adsorption capacity. On the other hand, the cross-linking reactions slightly decrease the adsorption capacity because some functional groups of chitosan (i.e., amino or hydroxyl groups) are linked with the cross-linker and cannot intermingle with the pollutant, that's why in more recent years researchers have attempted to prepare chitosan-based adsorbent materials modifying the molecules of chitosan [7]. The present work is on the modification of Chitosan/CMC composite with the cross-linker glutraldehyde and ethylene diamine and the study of cross-linkers effects on the adsorption capacity. To the best of our knowledge this article is the first article to report on using modified chitosan/CMC composites crosslinked with naturally occurring and environmentally friendly glutraldehyde and ethylene diammine cross-linkers for the removal of Cr (VI) from aqueous solutions at ambient conditions.

Materials and Methods

1. Chemicals

Chitosan with deacetylation of 93% (Moisture ≤ 10%, Faint Beige to Beige powder) was obtained from Oxford Lab Co., Ltd (India) and carboxymethyl cellulose sodium salt (High viscosity) was supplied by Trust Chemical Laboratories (TCL) (India) and they were used as received. Citric acid Monohydrate (2-hydroxy-1, 2, 3-propanetricarboxylic acid monohydrate, M.W. 210.14) was supplied from CDH Fine Chemicals (India). Acetic acid (99.5%, Extra Pure), was purchased from LOBA Chemie LABORATORY REAGENTS & FINE CHEMICALS (India). Sulfuric acid was obtained from CDH Fine Chemicals (India). 1, 5-diphenyl carbazide (m.p. 173-176oC, molecular mass=

242.28 g/mol) LabChem (USA). Acetone, CDH Fine Chemicals (India). Potassium dichromate (K2Cr2O7) was purchased from CDH Fine Chemicals (India). Glutaraldehyde solution 25%, (C5H8O2, glutaric dialdehyde 25% solution, Pentane 1,5-dial 25% solution) M.W 100.12) was purchased from SDFCL fine chemical limited. Ethylenediamine for synthesis (1, 2-Diaminoethane) NH2.CH2.CH2.NH2, M.W 60.10 was obtained from CDH Fine Chemicals (India).

2. Modification of chitosan/CMC composite

Take 0.5g of Chitosan carboxymethyl composite C11(DOI: 10.35629/5252-0311437451) in a 50ml of conical flask, add 25ml of distilled water in it and stir it on hot plate magnetic stirrer for 15 minutes. Add 2ml of glutraldehyde and stir it for 15 minutes. Add 3ml of ethylene diamine, stir it for 5 minutes, filter the solution, wash the residue with distilled water and let it dry at room temperature

3. Removal of Cr (VI) from aqueous solution using modified chitosan/CMC composites

For the preparation of 1000 ppm Stock solution of Cr (VI), 0.2829g of potassium dichromate was dissolved in distilled water in 1 liter volumetric flask and completes it till mark. From this stock solution of Cr (VI) another 50 ppm concentration standard solution of Cr (VI) was prepared and used for adsorption experiments. For the experiment, 10 ml of 50 ppm stock solution was taken into 50ml a plastic beaker and 0.02 g of modified composite was added and stirred well. The beaker with its content was left for 24 hours at ambient conditions and FTIR technique was used to determine the concentration of the remaining Cr (VI).

Fourier transform infrared analysis

The infrared spectra of CMC/chitosan composite and the modified composite were obtained using Fourier transform infrared spectrometer, FT-IR, Shimadzu (model 8400S - Japan). Few milligrams of the each sample were mixed thoroughly with sufficient amount of KBr and pressed to form a transparent disk. The infrared spectrum was recorded between 400 and 4000 cm-1 using a resolution of 4cm-1 and 8 numbers of scans.

Scanning electron microscopy

SEM was used to investigate the morphology of the modified composite sample through an InspectTM Scanning Electron Microscope (Inspect S50, Japan). The sample was frozen under liquid nitrogen, mounted, sputter-coated with gold and allowed to dry in a vacuum system. The dried sample was viewed using an accelerating voltage of 5.00 kV.

Thermogravimetric analysis

Thermogravimetric analysis was carried out using a Simultaneous Thermal Analyzer Neztsch STA449 F3 Jupiter. The analysis was carried out under nitrogen gas flow from room temperature to 700°C at a heating rate of 10°C/min.

Effect of time on removal of Cr (VI) from aqueous solutions

The effect of contact time on removal of Cr (VI) was studied by using modified composite. Contact times of 1, 2, 3, 4, 5, 7, 10, 12 and 15 minutes were selected to carry out the experimental work. Standard solution of Cr (VI) with 50 ppm concentration was prepared from stock solution (1000 ppm) of Cr (VI) and used for adsorption experiments. In a typical experiment, 10 ml of 50 ppm standard solution was taken into a plastic beaker and 0.02 g of composite was added and stirred well for 1 minute using a magnetic stirrer at ambient conditions and the remaining Cr (VI) was determined using UV/VIS spectrophotometry. Exactly typical steps were repeated but at different contact times of 2, 3, 4, 5, 7, 10, 12 and 15 minutes. A plot of the equilibrium adsorption capacity versus contact time was carried out.

Determination of Cr (VI) by UV/Visible spectrophotometry

The Cr (IV) concentration in aqueous solutions was determined by JENWAY 7205 UV/Visible-spectrophotometer at 540 nm by using 1, 5-diphenylcarbazide (DPC) method. Standard solution of Cr (VI) with 50 ppm concentration was prepared from 1000 ppm stock solution of Cr (VI). Series of standard Cr (VI) solutions having different concentrations of 0.2, 0.4, 0.5, 0.8, and 1 ppm were prepared from the 50 ppm stock solution of Cr (VI). 1.0 ml of each of the standard Cr(IV) was mixed with 9.0 ml of 0.2 M H2SO4 in a 10 ml volumetric flask then 0.2 ml of freshly prepared 0.25% (w/v) DPC in acetone was added into the volumetric flask. The mixture was stirred in a plastic beaker for 30s and then let to stand for 15 minutes for full color development. The absorbance of the colored solution was measured at λmax 540 nm using distilled water as a reference. The absorbance-concentrations calibration curve was plotted with a correlation coefficient, of 0.9998. For the adsorption experiment, 10 ml of 50 ppm Cr (IV) standard solution was taken into a conical flask and 0.02g of the modified composite sample was added. The content was stirred for 7 minutes and the concentration of the remaining Cr (IV) was determined following exactly the above given UV/Visible spectrophotometry method for the standard Cr (IV) solutions.

Absorbed Cr (VI) was calculated by equations 1 and 2:

$$q_e = \frac{(c_o - c_f)V}{m} \tag{1}$$

$$q_t = \frac{(c_o - c_t)V}{m} \tag{2}$$

Where qe is the equilibrium adsorption capacity, qt adsorption capacity at time t, Co and Cf are the initial and final C r(VI) concentrations, respectively, V is the volume of Cr (VI) solution in liter and m is the mass of the adsorbent in grams.

Effect of pH on removal of Cr (VI) from aqueous solutions

The effect of pH on the modified composite was determined at different pH values 2, 4, 6, 8 and 10. The Cr (VI) standard solution of 50 ppm concentration was prepared from 1000 ppm stock solution of Cr (VI) and used for adsorption experiments. In a typical experiment, 10 ml of 50 ppm standard solution was taken into 50 ml beaker and the pH was adjusted to 2, 4, 6, 8 and 10 using 0.1M NaOH or 0.1M HCl solutions with the aid of a pH-meter. 0.02 g of modified composite was added to contents of the beaker and stirred for 5 min on a magnetic stirrer at 150 rpm and then allowed to settle for 5 min to reach the equilibrium at ambient conditions. The remaining Cr (VI) was determined using UV/VIS spectrophotometry. A plot of the equilibrium adsorption capacity versus pH was carried out.

Effect of initial concentration of Cr (VI) on adsorption of Cr (VI) from aqueous solutions

The effect of initial concentration on adsorption of Cr (VI) was studied at different concentrations 10, 20, 30, 40, 50 and 70 ppm. Standard solution of Cr (VI) with 50 ppm concentration was prepared from stock solution (1000 ppm) of Cr (VI) and used for adsorption experiments. In a typical experiment, 10 ml of 10 ppm standard solution was taken into a 50 ml beaker and 0.02 g of the composite was added and stirred well for 7 minutes using a magnetic stirrer at pH 5 which was previously adjusted using 0.1M HCl or 0.1M NaOH with the aid of a pH-meter. The remaining Cr (VI) was determined using UV/VIS spectrophotometry. The whole experiment was repeated again but using 20, 30, 40, 50 and 70 ppm of Cr (VI) in each case.

Results and Discussion

FTIR analysis

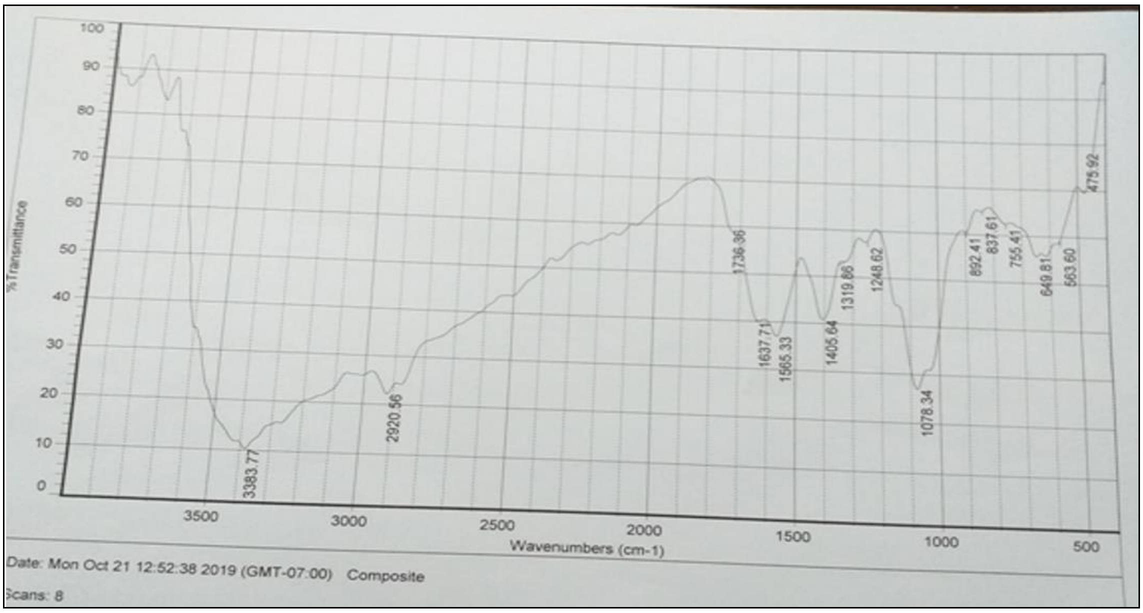

Fig 1: Chitosan/CMC Composite

Figure 1, shows the infrared spectrum of composite. The band at around 3000 to 3600 cm^{-1} could assign to aromatic secondary amine N-H and –OH stretching vibrations [8]. The absorption band at 2909 cm^{-1} is the C-H stretching vibration. The band at 1637 is due to the bending vibration of –OH group and the adsorption band at 1598 cm^{-1} shows the presence Of C=C asymmetrical stretches. The presence of symmetrical band C=C are confirmed by the bands at around 1637 cm^{-1} [9]. The presence of CH_2 and-C-N bands are attribute at around 1423 and 1382 cm^{-1}, respectively. The asymmetric stretching of the C-O-C bridge absorption band showed at 1149 cm^{-1} and the bands at 1095 and 1029 cm−1 correspond to C-O stretching. The band at 3398 cm^{-1} corresponds to O–H stretching vibrations. The band at 2918 cm^{-1} represents saturated C–H stretching vibration and the peak at 1075 cm^{-1} represent the C–O–C stretching vibration. The presence of a peak at 1736 cm^{-1} represents the formation of ester linkages [10].

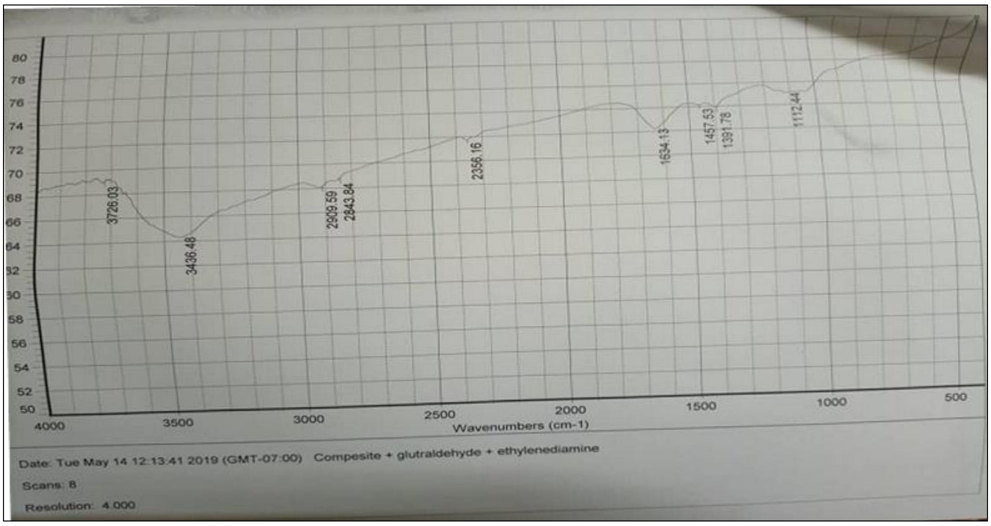

Fig 2: Modified Chitosan/CMC Composite (C11)

Figure 2 shows the FTIR spectrum of the modified composite. The comparison of composite and modified composite spectra showed that the peak area near 3200 cm^{-1} to 3450 cm^{-1} increased for the amino N-H and O-H groups. The peaks of 1033 cm^{-1} 1034 cm^{-1} and 1064 cm^{-1} corresponded to the C-O, while the peak at 1660 cm^{-1} was assigned to the carbonyl group of the amide [11]. On the other hand, it was observed that 3291 cm^{-1} (a wide O-H band), 2900cm^{-1}(aliphatic C-H stretching),2360cm^{-1} (C=C stretching) and 1634 cm^{-1}(N-H bending) are characteristic bands [12]. These results confirmed that amino groups were introduced onto the adsorbent surface and modified composite was successfully synthesized. In conclusion, the modified composite had more amino groups. The remaining peaks are typically similar to the ones that are shown already in Figure 1.

Scanning electron microscopy

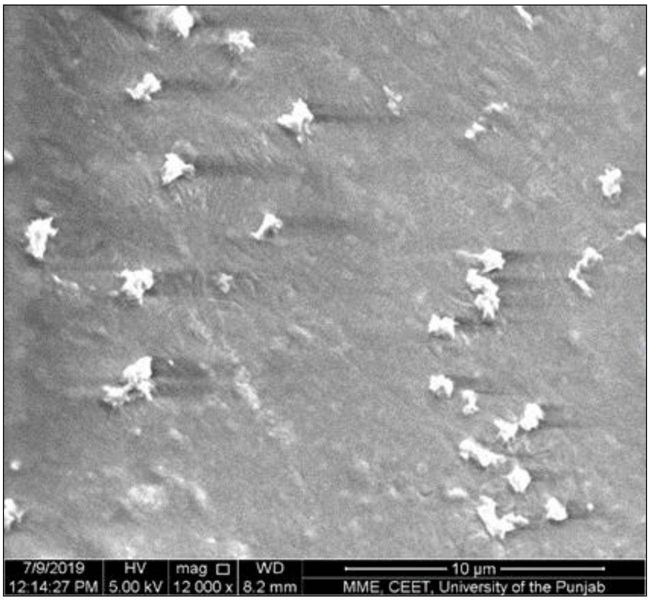

Fig 3

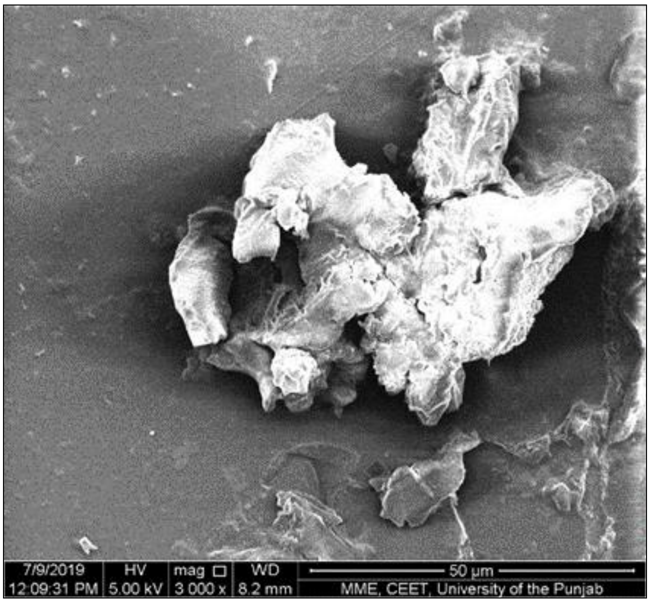

Fig 4

The SIM images(Figures 3,4) of surface morphology clearly showing the smooth surface with distributed cross linker groups on the surface of modified composite, the resulting the modified composite has strong affinity for the removal of chromium [13].

Thermo gravimetric analysis

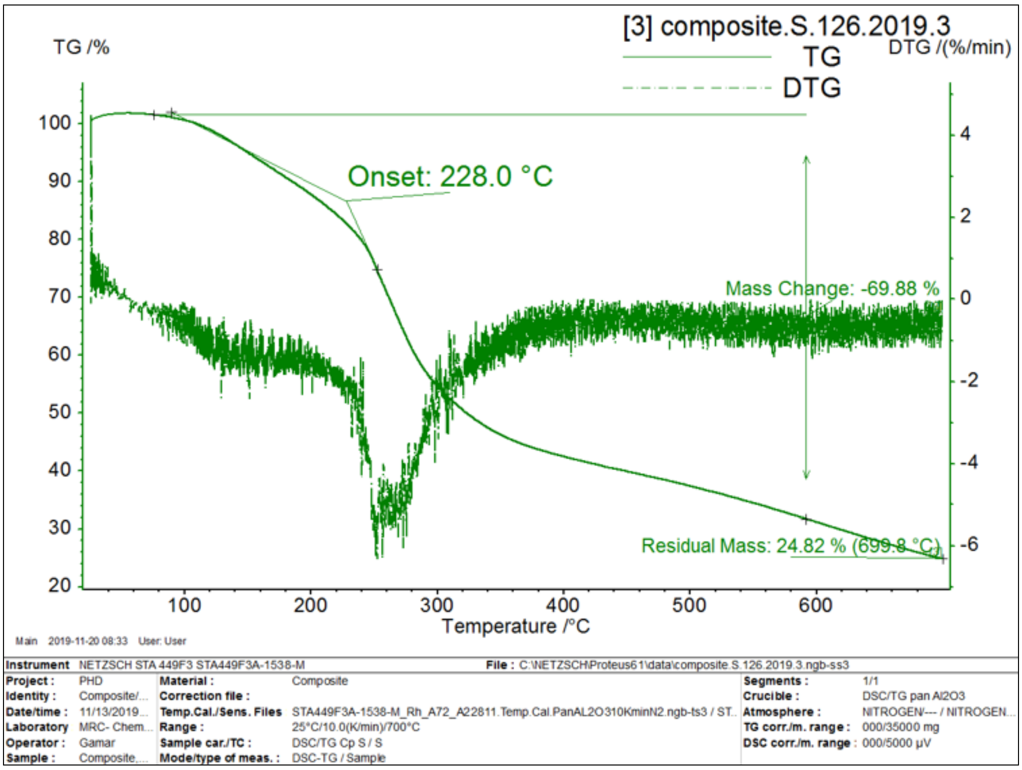

Instrument NETZSCH STA 449F3 STA449F3A-1538-M

File : C:\NETZSCH\Proteus61\data\composite.S.126.2019.3.ngb-ss3

Project : PHD
Identity : Composite/...
Date/time : 11/13/2019...
Laboratory MRC- Chem...
Operator : Gamar
Sample : Composite,...

Material : Composite
Correction file :
Temp.Cal./Sens. Files STA449F3A-1538-M_Rh_A72_A22811.Temp.Cal.PanAL2O310KminN2.ngb-ts3 / ST..
Range : 25°C/10.0(K/min)/700°C
Sample car./TC : DSC/TG Cp S / S
Mode/type of meas. : DSC-TG / Sample

Segments : 1/1
Crucible : DSC/TG pan Al2O3
Atmosphere : NITROGEN/--- / NITROGEN...
TG corr./m. range : 000/35000 mg
DSC corr./m. range : 000/5000 µV

Fig 5a

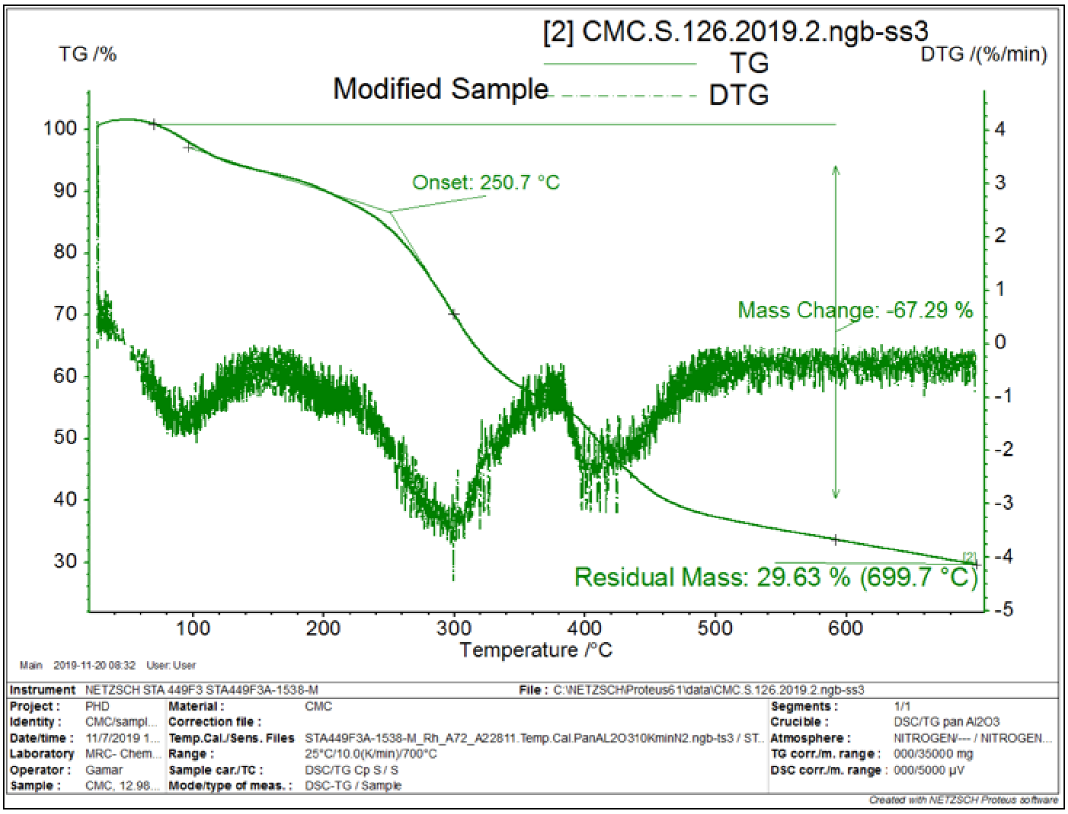

Instrument	NETZSCH STA 449F3 STA449F3A-1538-M	**File :**	C:\NETZSCH\Proteus61\data\CMC.S.126.2019.2.ngb-ss3		
Project :	PHD	**Material :**	CMC	**Segments :**	1/1
Identity :	CMC/sampl...	**Correction file :**		**Crucible :**	DSC/TG pan Al2O3
Date/time :	11/7/2019 1...	**Temp.Cal./Sens. Files**	STA449F3A-1538-M_Rh_A72_A22811.Temp.Cal.PanAL2O310KminN2.ngb-ts3 / ST...	**Atmosphere :**	NITROGEN/--- / NITROGEN...
Laboratory	MRC- Chem...	**Range :**	25°C/10.0(K/min)/700°C	**TG corr./m. range :**	000/35000 mg
Operator :	Gamar	**Sample car./TC :**	DSC/TG Cp S / S	**DSC corr./m. range :**	000/5000 µV
Sample :	CMC, 12.98...	**Mode/type of meas. :**	DSC-TG / Sample		

Fig 5b

In (Fig. 5a) the thermograms of composite in the temperature range of 30–600 °C shows few steps degradation. The first step takes place in the range of 30–100 °C. The small amount of weight loss occurs due to the loss of moisture contained in composite. In a second step the major degradation occur due to breakdown of polysaccharide structure in the range of 200 °C to 300 °C results in the weight loss of around 55% and the final loss of 25% gradually takes place in the range from 300 to 600 °C. Fig. 5b illustrates the clear degradation pattern of modified composite which is very different to that of composite. In the first step degradation about 10% of weight loss takes place in a temperature zone of 30–100 °C and is due to the loss of water molecules. In the second step, the weight loss is observed in the temperature zone of 200–300 °C and is due to the decomposition of the chitosan followed by decomposition of CMC in the temperature range of 300–600 °C. About 29% of the compound remained as residual matter and the changes in mass are decreased from 69 to 67% [14].

Effect of time on removal of Cr (VI) from aqueous solutions

The effect of time on removal of Cr (VI) from it is aqueous solutions were investigated using three different concentrations. The initial and the final concentrations of Cr (VI) were determined using UV/Visible spectrophotometry. The results are displayed in Figure 6. As can be seen from the Figure, the equilibrium adsorption capacity was increased with time gradually and reached its plateau between 6 to 8 minutes, so 7 minutes were chosen as the optimum time for adsorption experiments.

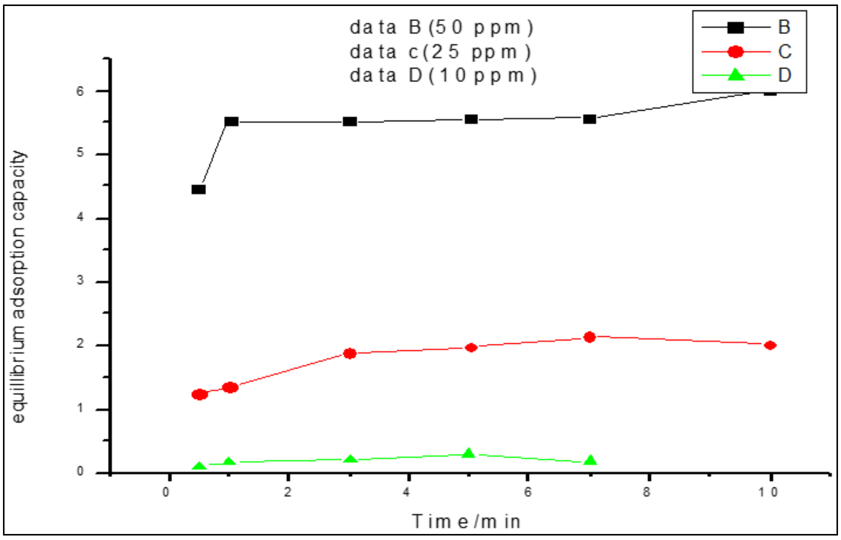

Fig 6: Effect of time on removal of Cr (VI)

Figure 6 illustrates the result of comparative study of contact time by using composite. It is evident that optimum contact time for the composite was found to be 7 min with maximum removal. The trend of percentage adsorption was shown that with increased contact time there is more time for the Cr (VI) to make complex with the adsorbent.

Effect of pH on removal of Cr (VI) from aqueous solutions

The effect of pH on removal of Cr (VI) from it is aqueous solutions were investigated using three different pH solutions. The results are displayed in Figures 7a and 7b. As can be seen from the Figure, the equilibrium adsorption capacity was increased with pH decreases and reached its maximum between 2 to 4 pH, as well as percentage removal is at its peak on PH 2. With increasing the pH level, the electrostatic repulsive forces between chromium ions and negative charge on the surface of the adsorbent becomes strong and resultant reduces the adsorption capacity [15]. The results of other researches similarly indicate the effect of the pH level on chromium adsorption capacity by different adsorbents [16, 17].

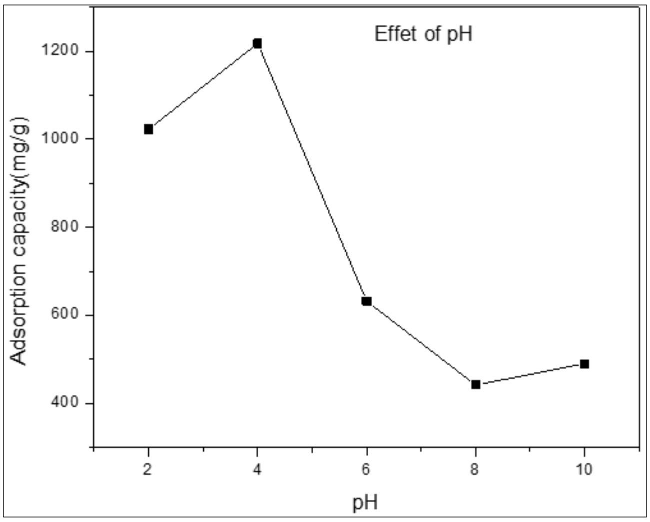

Fig 7a: Effect of PH on adsorption capacity

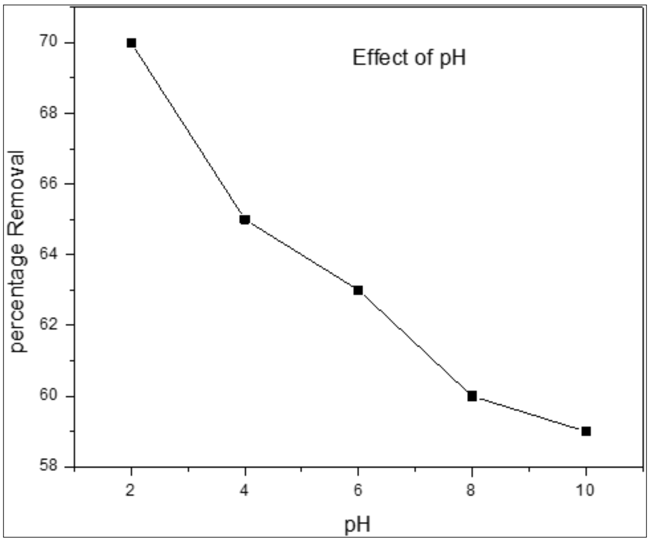

Fig 7b: effect of PH on Percentage removal

Adsorption isotherms

To study the relationship between absorbed amount (qe) and aqueous concentration (Ce) at equilibrium, adsorption isotherm models like Langmuir, Freundlich, Temkin and Dubinin-Radushkevich (DR) isotherm are widely working, in which Langmuir and Freundlich equations are most widely used [18]. The Langmuir model assumes that the uptake of adsorbate molecules occurs on a homogenous surface by monolayer adsorption without any interaction between adsorbed molecules. Freundlich model is suitable for non-ideal adsorption on heterogeneous surfaces. The heterogeneity is caused by the presence of different functional groups on the surface, and various adsorbent–adsorbate interactions [19]. The Langmuir isotherm is represented by equation 3.

$$\frac{Ce}{qe} = \frac{1}{KLqm} + \frac{Ce}{qm} \tag{3}$$

Equation 3, where qe was the quantity of Cr (VI) adsorbed per unit weight of adsorbent (mg/g) at equilibrium, Ce was the equilibrium concentration (mg/L) of Cr(VI) in solution. The constant q_m gives the theoretical monolayer adsorption capacity (mg/g).Straight lines were obtained by plotting Ce/qe against Ce as shown in Fig 2. The linear plot of Ce/qe against Ce indicated the applicability of Langmuir adsorption isotherm. Langmuir constants, qe and b were calculated from the slopes and intercepts of plots of Ce/qe versus Ce, respectively, and are given in Table 1 along with correlation coefficients (R2). The essential characteristics of the Langmuir isotherm can be expressed by a dimensionless equilibrium parameter, RL, also known as the separation factor to investigate the fundamental characteristics of the adsorption processes where an adsorption process is favorable (0<RL1), Linear (RL = 1), or irreversible (RL=0**)** [20].

$$RL = \frac{1}{1+KLCo} \tag{4}$$

Where KL describes the affinity of the surface for the solute and Co is the initial Cr (VI) concentration. The values of RL which indicated the favorable adsorption of Cr (VI) on the surface of modified composite. As shown in Table 1, the Langmuir model provides a determination coefficient (R2 = 0.911) higher than the other models, indicating the monolayer adsorption of Cr (IV) on modified composite. As shown in Figure 1, the RL value was 0.003, indicating the favorability of Cr (IV) adsorption on modified composite in the studied concentration range [21].

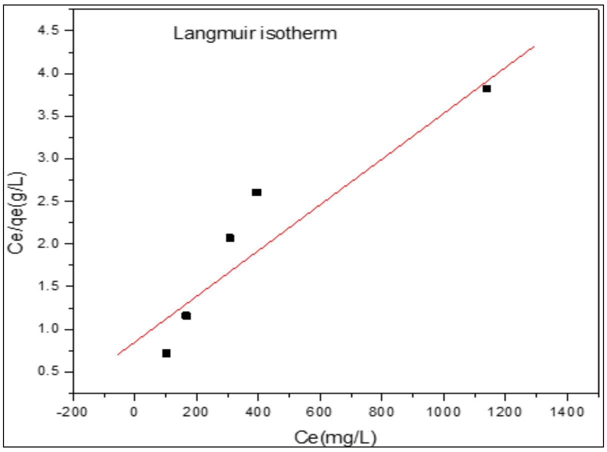

Fig 8: Langmuir adsorption isotherm

The Freundlich isotherm has the form

$$qe = Kf + 1/n\ Ce \qquad (5)$$

The logarithmic form of the equation is given below:

$$\log qe = \log Kf + 1/n \log Ce \qquad (6)$$

where qe is the uptake of metal per unit weight of biosorbent (mg/g), Ce the equilibrium concentration of metal ions in solution (mg/L), Kf the Freundlich constants denoting adsorption capacity (mg/g) and n is the empirical constant, indicating of adsorption intensity (L/mg). The value of Kf and 1/n were found by plotting the graph between log qe and logCe, which is the residual chromium concentration and is calculated from the laboratory data. The value of logKf is the intercept and value of 1/n is the slope of the plot. After finding the logKf, its antilog is found out to calculate Kf which was 0.326. A high 'Kf' and 'n' value is indication of chemical absorption throughout the concentration range. A low 'Kf' and high 'n' indicates physical adsorption throughout the studied concentration range [22]. The 'n' value (2.86) indicates physical good adsorption at strong solute concentration.

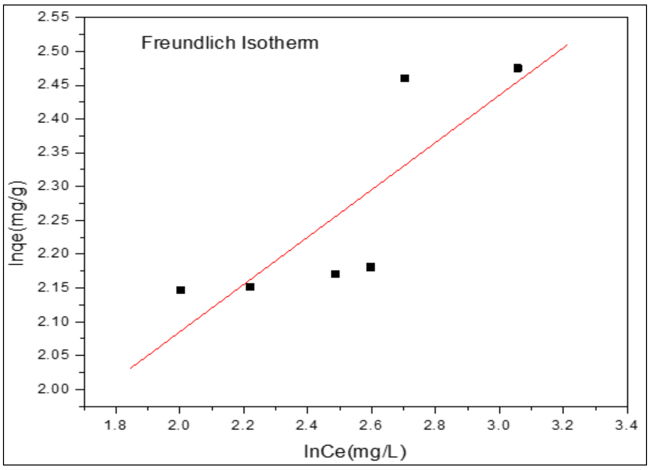

Fig 9: Freundlich adsorption isotherm

The Temkin isotherm model involves a factor that fully allows for including the interactions between adsorbents and adsorbates. Temkin model accepts the following conditions: (i) the adsorption heat of all molecules present in the layer linearly decreases with the coverage which is because of adsorbent–adsorbate interactions; (ii) a uniform distribution of binding energies, up to maximum binding energy, is used to characterize the adsorption [23]. The Temkin isotherm is commonly used in the form of following equation

$$qe = B \ln(KTCe) \qquad (7)$$

Where B = (RT/AT) and KT is Temkin constant. KT (J/mol) is the change of the Temkin adsorption energy between two neighboring adsorption sites, T (K) is the adsorption temperature and R (kJ/ mol K) is the universal gas constant. To simplify plotting and calculation of Temkin constant, the above equation is often rearranged as the linear form offered below. The values of KT and B can be calculated from the linear plot of qe versus ln(Ce).

$$qe = B \ln KT + B \ln Ce \qquad (8)$$

The linearized form of the Temkin adsorption isotherm presented (Eq. (8)) was used to analyze the equilibrium data and the data is shown in Table 1.

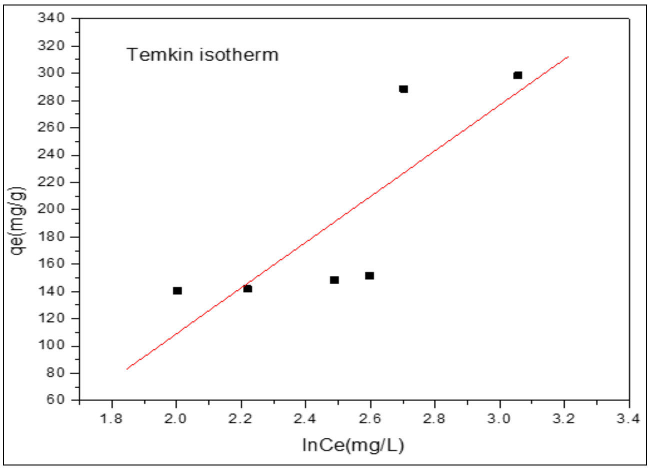

Fig 10: Temkin adsorption isotherm

The Dubinin–Radushkevich isotherm equation was used to distinguish between the chemical and physical adsorption [24]. The linear form of this model is expressed by:

$$lnqe=lnqm-K_{D\text{-}R}\,\varepsilon^{2} \qquad (9)$$

$$\varepsilon=RTCln(1+1/Ce) \qquad (10)$$

Where, qm (mg/g) is the D-R maximum biosorption and KD-R (mol^2 / kJ^2) shows the mean free energy of biosorption. The value of ε represents the Polanyi potential, R is the universal gas constant (8.314 J/mol/K) and T represents temperature in kelvin. The apparent energy of adsorption (E) (kJ/mol) was estimated using Eq. (11).

$$E\ K=1/\sqrt{2K} \qquad (11)$$

From the plots of ln qe versus ε^2 (Fig. 4) the values of Ek and qm were determined by the slope and intercept of the linear plot. The statistical results along with the isotherm constants are also given in Table 1. The magnitude of E gives information about the type of adsorption/ion exchange mechanism. E value lying between 1-8 kJ/mol indicates that the type of adsorption is physisorption while 8-16 kJ/mol specify ion exchange mechanism [25]. As our results showed, adsorption of Cr(VI) by modified composite was physisorbtion.

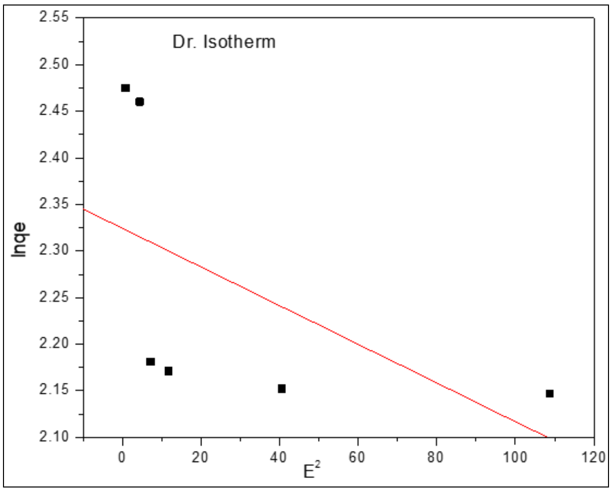

Fig 11: Dubinin-Radushkevich adsorption isotherm

Table 1: Different isotherm parameters for adsorption of Cr (VI) ions on modified composite at 293 K.

Langmuir isotherm parameters	
R2	0.9118
q_m (mg/g)	0.003
b (L/mg)	434.2
R_L	0.003
Freundlich isotherm parameters	
R2	0.8205
n	2.86
1/n	0.350
K_F (L/g)	0.326
Temkin isotherm parameters	
R2	0.8111
K_T (L/g)	0.300
β (J/mol)	167.8
DR isotherm models	
R2	0.5469
E_S (kJ/mol)	15.63
Langmuir isotherm parameters	

Adsorption kinetics

The amount of metal ion adsorbed by the adsorbent depends on the contact time and thus, kinetics of adsorption of Cr (VI) was explained through pseudo-first-order and pseudo-second order kinetic intraparticle diffusion and Elovich kinetics models. The studies were carried out using different concentrations of Cr (VI) solution *viz.* 10, 20,30,40,50,60 and 70 mg/L. The solutions were equilibrated with 0.02 g/L of adsorbent at 298 K and pH 4.0 for different time intervals (1-7 min). The results obtained have been summarized in Table 2.The pseudo-first-order kinetics is given by the equation

$$\text{Log (qe-qt)} = \log qe - \frac{K1}{2.303}\,t \qquad (12)$$

Where qe and qt refer to the amounts of Cr(VI) adsorbed at equilibrium and at time t with the first- order rate constant k1.The plot of log (qe – qt) against t gives pseudo-first-order rate constant Fig. 12 [26].

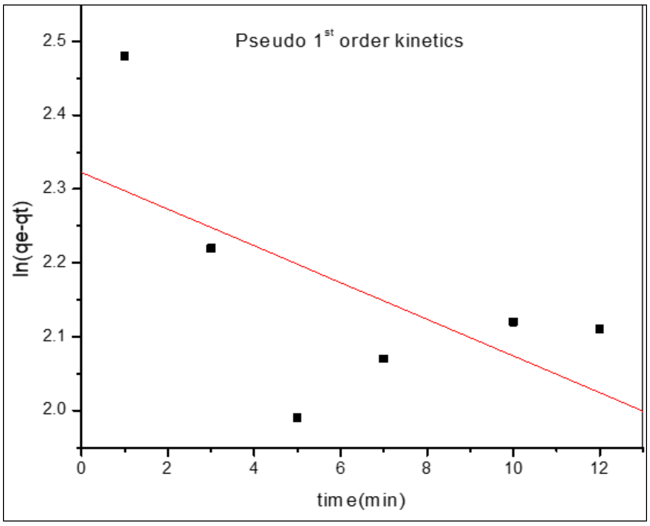

Fig 12: Pseudo 1st order

The pseudo-second-order equation is given as

$$\frac{t}{q1} = \frac{1}{K2qo} + \frac{1}{qe}t \qquad (13)$$

Where k_2 is the pseudo-second-order rate constant in g/mg/min. For all the concentrations, the plot of log t/qt against t gives pseudo-second-order rate constant Fig. 13. From Table 2 it is cleared that the values of experimental qe obtained in pseudo-second-order rate model had close agreement with that of calculated qe indicating the fitment of experimental data in pseudo-second- order rate model [27].

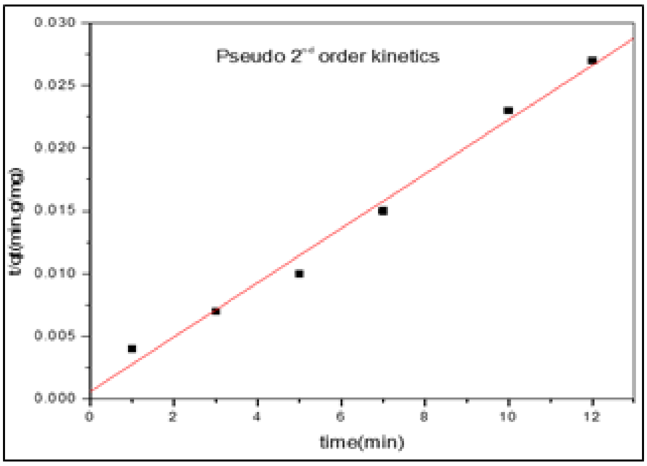

Fig 13: Pseudo 2nd order

During adsorption, whether intraparticle diffusion is the rate determining step can be confirmed by Weber–Morris model (Weber & Morris, 1963).

$$qt = kpt^{1/2} + c \qquad (14)$$

Where kpt is the intra-particle diffusion rate constant (mg/g min1/2), and the value of C (mg/g) represents the thickness of the boundary layer. In the case of the intra-particle diffusion model, the increase in the C values with an increase in initial Cr(VI) concentrations corresponds to the increase in boundary layer thickness, and the resistance to the external mass transfer increases. The linear plot was not passed through the origin Fig 14 indicating that the intra-particle diffusion was not the only rate controlling step and some other mechanism presided over the Cr(VI) adsorption process along with intra-particle diffusion [28].

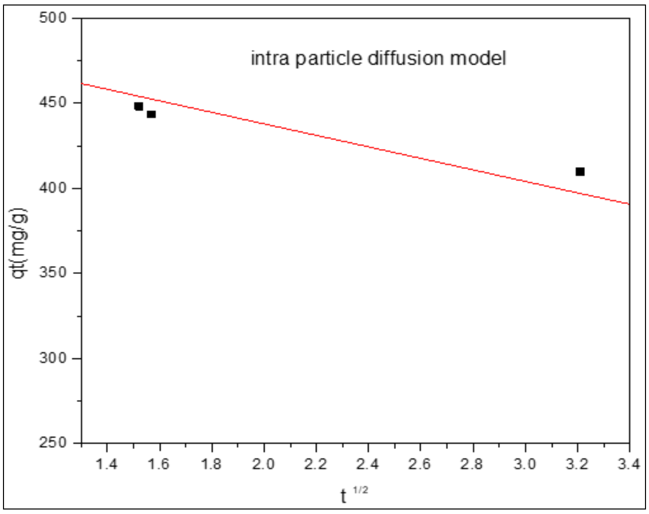

Fig 14: Intra-particle diffusion

The Elovich model which assumes multilayer adsorption is given by the expression

$$\ln\frac{q_e}{c_e} = \ln K_E\, q_m - \frac{q_e}{q_m} \quad (15)$$

$$q = (1/\beta)\ln(\alpha\beta) + (1/\beta)\ln t \quad (16)$$

Where KE and qm are characteristic of the Elovich equilibrium constant and the adsorption capacity, α represents the rate of chemisorption at zero coverage (mg g1 min1) and β is related to the extent of surface coverage and activation energy for chemisorption (g mg1). These constants were calculated from the slope and intercept of the plots of q vs lnt (Fig. 15). This suggests that the sorption systems studied belong to the second order kinetic model based on the assumption that the rate determining step may be chemisorption involving valence forces through sharing or exchange of electrons between adsorbent and adsorbate. The relevant Elovich isotherm parameters are obtained from the Elovich plot relating ln (qe/Ce) against qe given in Table 1 [29].

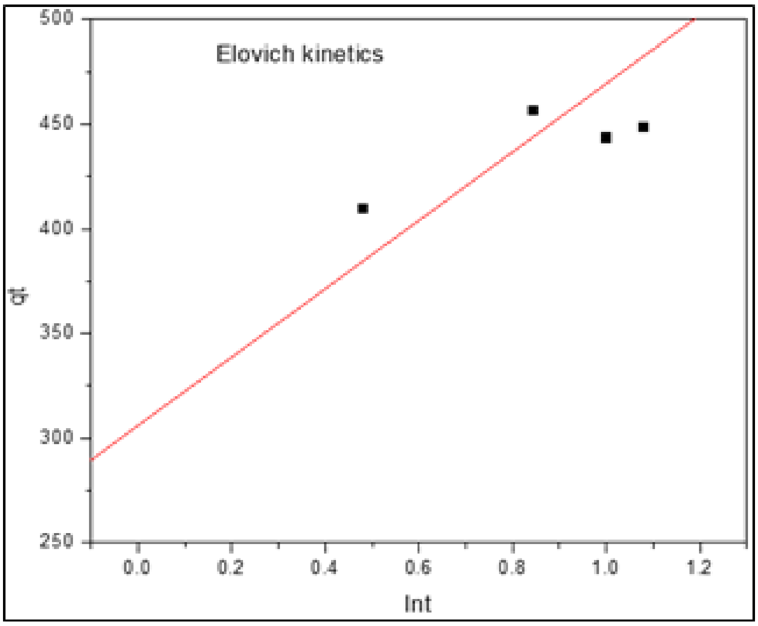

Fig 15: Elovich Kinetics

Table 2: Kinetic parameters for adsorption of Cr (VI) ions on modified composite

Pseudo 1st order	
R2	0.6057
qe (mg/g)	0.366
k1 (min−1)	0.0248
Pseudo 2nd order	
R2	
qe (mg/g)	3.67
h (mg/g·min)	0.029
t1/2 (min)	123.9
k2 (g/mg·min)	0.021
Intra-particles diffusion model	
R2	0.3686
C (mg/g)	33.77
kipd (mg/g·min)	4.08
Elovich model	
R2	0.8645
α (mg/g·min)	2.49
β (g/mg)	163.4

Conclusion

In conclusion, the resultant modified composites had more adsorbent properties than C11 composite with the reference DOI: 10.35629/5252-0311437451 and it was used to remove Cr (VI) from standard aqueous solution, and characterized by the FT-IR, SEM and TGA. The optimum conditions for adsorption of Cr (VI) on modified composite were found at pH range of 2.0-4.0 and stirring time of 7 minutes. Kinetic study results showed that the adsorption process follows pseudo-second order model, while the Langmuir adsorption isotherm provide the best fit with a maximum adsorption capacity from 33.77 to 89.24 mg/g at 25oC, indicating that the rate limiting step in the absorption of Cr (IV) involves the best physical interaction physisorption. Thermodynamic parameters in TGA analysis indicated an endothermic process and spontaneous adsorption of Cr (VI) on the polymers.

References

1. Campos EV, Oliveira JL, Fraceto LF. Poly (ethylene glycol) and cyclodextrin-grafted chitosan: From methodologies to preparation and potential biotechnological applications. Frontiers in chemistry,2017:5:93.
2. Bi S, Hu S, Zhou Z, Kong M, Liu Y, Feng C *et al*. The green and stable dissolving system based on KOH/urea for homogeneous chemical modification of chitosan. International journal of biological macromolecules,2018:120:1103-1110.
3. Saheed IO, Da OW, Suah FBM. Chitosan Modifications for Adsorption of Pollutants-A review. Journal of Hazardous Materials, 2020, 124889.
4. Javadian H, Ruiz M, Saleh TA, Sastre AM. Ca-alginate/carboxymethyl chitosan/Ni0. 2Zn0. 2Fe2. 6O4 magnetic bionanocomposite: Synthesis, characterization and application for single adsorption of Nd+ 3, Tb+ 3, and Dy+ 3 rare earth elements from aqueous media. Journal of Molecular Liquids,2020:306:112760.
5. Borsagli FGLM, Borsagli A. Chemically modified chitosan bio-sorbents for the competitive complexation of heavy metals ions: a potential model for the

treatment of wastewaters and industrial spills. Journal of Polymers and the Environment,2019:27(7):1542-1556.

6. Kanmani P, Aravind J, Kamaraj M, Sureshbabu P, Karthikeyan S. Environmental applications of chitosan and cellulosic biopolymers: A comprehensive outlook. Bioresource Technology,2017:242:295-303.
7. Elsabee MZ, Abdou ES, Nagy KS, Eweis M. Surface modification of polypropylene films by chitosan and chitosan/pectin multilayer. Carbohydrate Polymers,2008:71(2):187-195.
8. Kyzas GZ, Bikiaris DN. Recent modifications of chitosan for adsorption applications: a critical and systematic review. Marine drugs,2015:13(1):312-337.
9. Zhang H, Ma J, Wang F, Chu Y, Yang L, Xia M. Mechanism of carboxymethyl chitosan hybrid montmorillonite and adsorption of Pb (II) and Congo red by CMC-MMT organic-inorganic hybrid composite. International journal of biological macromolecules,2020:149:1161-1169.
10. Zhou L, Ouyang J, Shehzad H, Le Z, Li Z, Adesina AA. Adsorption of U (VI) onto the carboxymethylated chitosan/Na-bentonite membranes: kinetic, isothermic and thermodynamic studies. Journal of Radioanalytical and Nuclear Chemistry,2018:317(3):1377-1385.
11. Bagheri N, Lakouraj MM, Hasantabar V, Mohseni M. Biodegradable macro-porous CMC-polyaniline hydrogel: synthesis, characterization and study of microbial elimination and sorption capacity of dyes from waste water. Journal of Hazardous Materials,2021:403:123631.
12. de Andrade Neto JC, Pereira GJ, Morandim-Giannetti ADA. Chitosan and corn stover derivative bioadsorbent: characterization and application in hexavalent chromium adsorption processes. Cellulose,2020:27:6317-6331.
13. Huang Z, Huang Z, Feng L, Luo X, Wu P, Cui L, Mao X. Modified cellulose by polyethyleneimine and ethylenediamine with induced Cu (II) and Pb (II) adsorption potentialities. Carbohydrate polymers,2018:202:470-478.
14. Guo DM, An QD, Xiao ZY, Zhai SR, Shi Z. Polyethylenimine-functionalized cellulose aerogel beads for efficient dynamic removal of chromium (VI) from aqueous solution. RSC advances,2017:7(85):54039-54052.
15. Altun T. Preparation and application of glutaraldehyde Cross-linked chitosan coated bentonite clay capsules: chromium (VI) removal from aqueous solution. Journal of the Chilean Chemical Society,2020:65(2):4790-4797.
16. Mohamed A, Nasser WS, Osman TA, Toprak MS, Muhammed M, Uheida A. Removal of chromium (VI) from aqueous solutions using surface modified composite nanofibers. Journal of colloid and interface science,2017:505:682-691.
17. Anush SM, Vishalakshi B. Modified chitosan gel incorporated with magnetic nanoparticle for removal of Cu (II) and Cr (VI) from aqueous solution. International journal of biological macromolecules,2019:133:1051-1062.
18. Al-Othman ZA, Ali R, Naushad M. Hexavalent chromium removal from aqueous medium by activated carbon prepared from peanut shell: adsorption kinetics, equilibrium and thermodynamic studies. Chemical Engineering Journal, 2012:184:238-247.
19. Anupam K, Dutta S, Bhattacharjee C, Datta S. Adsorptive removal of chromium (VI) from aqueous solution over powdered activated carbon: Optimisation through response surface methodology. Chemical Engineering Journal,2011:173(1):135-143.
20. Khosravi R, Moussavi G, Ghaneian MT, Ehrampoush MH, Barikbin B, Ebrahimi AA *et al*. Chromium adsorption from aqueous solution using novel green nanocomposite: adsorbent characterization, isotherm, kinetic and thermodynamic investigation. Journal of Molecular Liquids,2018:256:163-174.
21. Wang XS, Li ZZ, Tao SR. Removal of chromium (VI) from aqueous solution using walnut hull. Journal of Environmental Management,2009:90(2):721-729.
22. Vimonses V, Lei S, Jin B, Chow CW, Saint C. Kinetic study and equilibrium isotherm analysis of Congo Red adsorption by clay materials. Chemical Engineering Journal,2009:148(2-3):354-364.
23. Asl SH, Ahmadi M, Ghiasvand M, Tardast A, Katal R. Artificial neural network (ANN) approach for modeling of Cr (VI) adsorption from aqueous solution by zeolite prepared from raw fly ash (ZFA). Journal of Industrial and Engineering Chemistry,2013:19(3):1044-1055.
24. Bazzazzadeh R, Soudi MR, Valinassab T, Moradlou O. Kinetics and equilibrium studies on biosorption of hexavalent chromium from leather tanning wastewater by Sargassum tenerrimum from Chabahar-Bay Iran. Algal Research,2020:48:101896.
25. Preethi J, Prabhu SM, Meenakshi S. Effective adsorption of hexavalent chromium using biopolymer assisted oxyhydroxide materials from aqueous solution. Reactive and Functional Polymers,2017:117:16-24.
26. Kahu SS, Shekhawat A, Saravanan D, Jugade RM. Two fold modified chitosan for enhanced adsorption of hexavalent chromium from simulated wastewater and industrial effluents. Carbohydrate polymers,2016:146:264-273.
27. Boddu VM, Abburi K, Talbott JL, Smith ED. Removal of hexavalent chromium from wastewater using a new composite chitosan biosorbent. Environmental science & technology,2003:37(19):4449-4456.
28. Dai J, Ren F, Tao C. Adsorption of Cr (VI) and speciation of Cr (VI) and Cr (III) in aqueous solutions using chemically modified chitosan. International journal of environmental research and public health,2012:9(5):1757-1770
29. Rangabhashiyam S, Selvaraju N. Efficacy of unmodified and chemically modified Swietenia mahagoni shells for the removal of hexavalent chromium from simulated wastewater. Journal of Molecular liquids,2015:209:487-497
30. Kumar ASK, Ramachandran R, Kalidhasan S, Rajesh V, Rajesh N. Potential application of dodecylamine modified sodium montmorillonite as an effective adsorbent for hexavalent chromium. Chemical Engineering Journal,2012:211:396-405.
31. Namasivayam C, Sureshkumar MV. Removal of chromium (VI) from water and wastewater using surfactant modified coconut coir pith as a biosorbent. Bioresource technology,2008:99(7):2218-2225.